

X-ray Study of Seventy-nine Distant Clusters of Galaxies: Discovery of Two Classes of Cluster Size

Naomi Ota^{1,2,3} and Kazuhisa Mitsuda³

ABSTRACT

We have performed a uniform analysis of 79 clusters of galaxies with the ROSAT HRI and ASCA to study the X-ray structure and evolution of clusters in the redshift range $0.1 < z < 1$. We determined the average X-ray temperatures and the bolometric luminosities with ASCA and the spatial distributions of the X-ray brightness with the ROSAT HRI by utilizing the isothermal β -model. We do not find any significant redshift dependence in the X-ray parameters including the temperature, β -model parameters, and the central electron density. Among the parameters, the core radius shows the largest cluster-to-cluster dispersions. We discovered that the histogram of the core radius shows two peaks at 60 and 220 kpc. If we divide the cluster samples into two subgroups corresponding to the two peaks in the core radius distribution, they show differences in the X-ray and optical morphologies and in the X-ray luminosity-temperature relation. From these observational results, we suggest that the clusters are divided into at least two subgroups according to the core radius.

Subject headings: Galaxies:Clusters – X-Rays:Galaxies – Cosmology:Dark Matter

1. Introduction

Clusters of galaxies are the largest collapsed structures in the universe, and thus are a useful cosmological probe. At X-ray energies, thermal emission from highly ionized plasma that is confined in the cluster is an excellent tracer of the underlying gravitational potential. A large number of cluster samples observed with the ASCA and ROSAT observatories enable us to investigate both the spatial and spectral structures systematically. Mohr, Mathiesen, &

¹Department of Physics, Tokyo Metropolitan University, 1-1 Minami-osawa, Hachioji, Tokyo 192-0397, Japan

²naomi@phys.metro-u.ac.jp

³Institute of Space and Astronautical Science, Sagami-hara, Kanagawa 229-8510, Japan

Evrard (1999) performed a uniform analysis on the ROSAT PSPC data of forty-five clusters with $z \lesssim 0.1$ under the β -model (Cavaliere & Fusco-Femiano 1976) and gathered the spectral data from the literature. Based on their results, Fujita & Takahara (1999a) found that the nearby clusters show a planar distribution in the 3-dimensional parameter space, and named it the X-ray fundamental plane. Fujita & Takahara (1999b) proposed that the major axis of the plane may represent the cluster formation epoch. According to their interpretations, the distributions of more distant clusters on the plane should be displaced in comparison to the nearby samples.

In order to constrain structure and evolution of clusters, it is important to extend the cluster study to a wider redshift range. However, at $z > 0.1$, only a limited number of clusters have been uniformly analyzed (e.g. Allen (1998); Ettori & Fabian (1999); Hashimoto-dani (1999)). In this paper and Ota (2001), we analyzed the ROSAT HRI and the ASCA SIS/GIS data of 79 clusters in a uniform manner for the first time. The analysis includes the largest sample of pointed observations of distant clusters. We report on the results of the redshift dependence of the X-ray properties and the double structure discovered in the spatial distributions of the intracluster gas. We use $H_0 = 50$ km/s/Mpc, $\Omega_M = 0.3$, and $\Omega_\Lambda = 0.7$ throughout the paper.

2. Systematic analysis

2.1. The sample

We have selected distant clusters with $0.1 < z < 1$ for which both ASCA and the ROSAT HRI pointed observations were made. Excluding three clusters that were observed away from the center of the field of view of the ROSAT HRI, the sample comprises 79 clusters. Clusters with $z < 0.4$ make up about 90% of the sample. Since the samples are collected from proposal observations, and also since the sensitivities for high-redshift clusters are limited, we have to be careful about selection bias. Our sample covers the temperature range almost equivalent to that of the X-ray flux limited 55 cluster sample constructed by Edge et al. (1990), but has a higher average temperature of 6.8 keV. The K-S test shows the probability that the two samples are from the same temperature distribution is 0.06 (the K-S parameter, $D = 0.24$). Observation bias will be discussed in a later section in more detail.

2.2. Spatial analysis

We have made use of the ROSAT Data Archive of the Max-Planck-Institut für extraterrestrische Physik to study the spatial distributions. We used the EXSAS analysis package (Zimmermann et al. 1992) to produce the HRI images from the event lists and rebinned the images into $5''$ bins. We first exclude image regions of point sources that were detected by the maximum likelihood method. Then we define the cluster center as the center of gravity of the photon distribution in a given aperture radius, and derive azimuthally averaged radial profiles. We fit the radial profiles with the isothermal β -model to determine the best-fit model parameters that minimize χ^2 . The single β -model fitting function is written as $S(r) = S_0(1 + (r/r_c)^2)^{-3\beta+1/2} + C$, where S_0 , r_c , and β are the central surface brightness, the core radius and the outer slope, respectively, and C is a constant background.

In order to estimate the possible systematic errors, we studied the dependence of the best-fit parameter values on analysis parameters; the aperture radius for the cluster centroid determination, and the inner and outer radii of the image region used in the model fittings.

The centroid positions of 34 clusters showed significant (more than 3σ) variations as a function of the aperture radius of the centroid determination compared to the statistical errors estimated by Monte-Carlo simulations. We find the variation is due to irregularity of the photon distribution. Thus we define the 34 clusters as “irregular” clusters, and the others as “regular” clusters. However, even for the irregular clusters, the deviations of the best-fit β -model parameters due to the selection of the aperture radius were smaller than the statistical errors, as long as the aperture radius is large enough that there is no significant cluster emission outside it but it is smaller than $12'$, within which radial dependences of telescope vignetting and background are small (Snowden 1998).

If the outer radius used for the fitting is too small, we overestimate or underestimate the background level and introduce systematic errors in the fitting parameters. However, we find the best-fit values are constant within the statistical errors as long as the outer radius is large enough, but $\lesssim 12'$.

The fit significantly improved for nine “regular” clusters when we excluded a few central bins from the fitting. We restricted this analysis to the regular clusters to avoid apparent double structure that could arise from the irregularities. The best-fit core radius increased for seven of them when we excluded the central bins. This indicates that those clusters contain two different length scales. Thus we define the double β -model as a superposition of two single β -models with different core radii. For all the nine clusters, the radial profiles are better fitted with the double β -model than the single β -model; the improvement is significant by the F-test at the 95% level. We refer to those nine clusters as the double- β clusters hereafter. Of

these, we classify seven clusters as inner-core dominant double- β , because the central surface brightness of the inner-core component is higher by one to two orders of magnitude than that of the outer-core component. We call the remaining two clusters outer-core dominant double- β , because the outer-core component dominates the total luminosity.

2.3. Spectral analysis

We integrated the cluster spectra from the circular regions of radius $3'$ for the SIS and $6'$ for the GIS. We subtracted the background spectra that were obtained through blank sky observations. Assuming a thin-thermal emission model (Raymond & Smith 1977), we fitted the SIS and GIS spectra simultaneously, where the absorption column density was allowed to vary in order to take into account the uncertainty in the low energy efficiency of the SIS detector (Yaqoob 1999). We determined the emission-weighted average temperature, kT and also estimated the bolometric luminosity, $L_{X,\text{bol}}$. We evaluated systematic errors caused by the selection of integration area and the background subtraction in the analysis, and found they are smaller than the statistical errors. We checked the consistency of the luminosities from ASCA and ROSAT. We find the luminosity from the HRI surface brightness profile is systematically higher by about 15%. We consider that this is within calibration errors of the effective areas of the X-ray telescopes (Fukazawa et al. (1997); Prestwitt et al. (1998))

3. Results

3.1. Redshift dependence

In Figure 1, we plotted the redshift dependence of the average temperature and core radius obtained from the present analysis together with the data for clusters with $z \lesssim 0.1$ from Mohr, Mathiesen, & Evrard (1999). With three overlaps there are 121 clusters. We do not find many clusters with $kT < 5$ keV at $z > 0.4$. As indicated in Figure 1 (a), this is consistent with the ASCA sensitivity, if we assume the luminosity-temperature relation of the clusters (See subsection 3.3). We also do not find many clusters with a core radius larger than ~ 300 kpc or smaller than ~ 40 kpc at $z > 0.4$. This is again consistent with the selection effect, because the detection of clusters with very small and large core sizes are limited respectively by the spatial resolution ($5''$) and by the sensitivity for low surface brightness emission (see sensitivity curves in Figure 1 (b)). Therefore, due to the sensitivity limit, the redshift evolution of the temperature and the core radius is not clear, although there is large cluster-to-cluster scatter. We also found that β and the central electron density

have no significant redshift dependence either. The average and the standard deviation of β for the 79 samples are 0.65 and 0.29, respectively.

It is remarkable that the core radius shows the largest cluster-cluster dispersions among the X-ray parameters, spanning over an order of magnitude. We also notice in Figure 1 (b) that the number of clusters with $r_c \sim 100$ kpc is smaller compared to clusters with $r_c \sim 50$ and 200 kpc.

The fraction of the irregular clusters in our sample is 43%. This is smaller than the fractions of irregular clusters of nearby clusters; 71% for 46 Einstein IPC samples (Mohr et al. 1995), 49% of 39 ROSAT PSPC samples (result with a $1 h_{80}^{-1}$ Mpc aperture in Buote & Tsai (1996)). All the substructure tests measure departures from regularity against the level expected from Poisson noise. The typical number of photons of our cluster sample is by a factor of ~ 2 smaller than that of the nearby sample of Mohr et al. (1995). Thus this may partly account for the difference. Difference in analysis techniques to quantify irregularities and selection bias may also partly explain the difference.

3.2. Core radius distribution

In Figure 2 we show histograms of the core radius for the single- β and the double- β clusters, separately. In the histograms we included the nearby clusters of Mohr, Mathiesen, & Evrard (1999). Eighteen of their samples are better fitted with the double β -model. For the single- β clusters, there are clearly two peaks at 60 kpc and 220 kpc. They are separated by about a factor of 4 and the depletion around 100 kpc is significant at the 4σ level if the population is comparable to those in the two peaks. About 70% of clusters (64 out of 95) are within two core-radius ranges corresponding to the peaks: $40 < r_c < 80$ kpc and $160 < r_c < 320$ kpc. Although the detection of large and small core clusters are seriously affected by the selection effect at $z > 0.4$, there is no reason that makes the detection of the intermediate core sizes of ~ 100 kpc difficult and it is very unlikely that the proposers of those observations avoided clusters of the intermediate core size. Therefore, as the observed double-peaked distribution cannot be explained by selection effects, it reflects the real nature of the clusters. For the double- β clusters, the inner core and the outer core are distributed around 60 kpc and 250 kpc, respectively. The coincidence with the two peak values of the single- β clusters is also striking.

3.3. Optical morphology and $L_X - T$ relation

In Figure 1, we find a systematic difference in r_c between the regular and the irregular clusters; clusters with a small (large) core tend to have a regular (irregular) X-ray morphology. Furthermore, among 37 clusters for which the optical Bautz-Morgan type is known, all 6 clusters classified as BM I or I-II (i.e. a cluster with a cD galaxy) are found to be either a single- β cluster with a small core or a double- β cluster.

Concentrated gas distribution in the small core system is indicated from the plot of the $L_X - T$ relation (Figure 3). The clusters with $r_c < 135$ kpc and > 135 kpc are denoted by different symbols. The core radius of the dominant core was used for the classification of the double- β clusters. We obtained the observed $L_X - T$ relations of the form $\log kT = a(\log L_{X,\text{bol}} - 45.4) + b$ with $(a, b) = (0.37 \pm 0.12, 0.68 \pm 0.04)$ for $r_c < 135$ kpc and $(a, b) = (0.324 \pm 0.097, 0.81 \pm 0.03)$ for $r_c > 135$ kpc, where the errors (90%) were estimated from the dispersion of the data points around the model function rather than the photon statistics. Thus the slopes are consistent for the two subgroups, however, the offsets differ significantly. The difference is consistent with a higher central electron density for the small core group: we find from the β -model analysis that n_{e0} is approximately related to r_c through $n_{e0} \propto r_c^{-\alpha}$ with $\alpha \sim 1.5$. Fabian et al. (1994) mentioned that the offset of clusters from the mean $L_X - T$ relation can be explained by the strength of cooling flow. We discuss the connection between the double peak structure of the core radius distribution and the $L_X - T$ relation in more detail in a separate paper (Mitsuda & Ota 2002).

4. Discussion

We found that among the X-ray parameters, the core radius has the largest scatter and that its histogram shows a double-peaked distribution. The optical and X-ray morphologies and the $L_X - T$ relation show correlations with the core radius. These results indicate that the clusters are divided into two subgroups according to the core radius.

In some nearby clusters, a central concentration in the iron distribution has been detected (e.g. Ezawa et al. (1997)). This may enhance the central surface brightness and might produce a double- β profile. We generated simulated single- β cluster images assuming the abundance gradient profile observed for AWM7 in which the abundance increases from 0.2 to 0.5 solar toward the center, and the average temperature from 0.5 to 3 keV. When the temperature is 3 keV, the central excess emission attributed to the gradient is only about 10% and the radial profile is well fitted with the single β -model. When kT is lower than 1 keV, the radial profile approaches that of the outer core dominant double- β cluster. Thus

the outer core dominant double- β clusters can be explained by simultaneous abundance and temperature gradients, because although the observed average temperatures are all higher than 2 keV, the temperature of the inner core region can be lower for outer core dominant double- β clusters. However, the inner-core dominant double- β clusters cannot be explained with this model.

Because of the similarity of the core radius distributions between the single- β and the double- β clusters, we tested the assumption that the clusters classified as the single- β regular clusters also contain a double- β profile within the photon statistics, assuming the ratio of the two core radii to be 1 : 4, and the ratio of central surface brightnesses 1 : 0.01 to 1 : 1. As a result, we found that the double β -model cannot be rejected at the 90 % level for about 2/3 of the single- β regular clusters. Thus it is possible that a large fraction of the clusters contain two different length scales in X-ray brightness distribution and can be approximated with the double β -model. The fraction of double- β clusters in nearby regular clusters (Mohr et al. 1995; Mohr, Mathiesen, & Evrard 1999) is $\sim 60\%$ (4 out of 7 regular clusters). Thus the fractions are consistent for the distant and the nearby samples.

The radiative cooling timescale at the cluster center is shorter than the age of the universe for most of the small core clusters. This supports the presence of the cooling flow phenomenon (e.g. Fabian (1994)). The cooling flow model predicts the emergence of a cool component at the cluster center. If the small core radius of the small-core subgroup is due to such a cool component, these clusters should contain another emission component of a larger core radius which reflects the gravitational potential. From the upper limit of the surface brightness of the outer component from the analysis in the previous paragraph, we find the photon flux from the outer component is smaller than 25% of the total emission for most of clusters of the subgroup. Thus the average cluster temperature should reflect the average temperature of the central enhancement. However we do not observe a strong correlation between r_c and kT . In particular, the temperature ranges of clusters with $r_c < 135$ and $r_c > 135$ kpc are comparable to each other (see Figure 3). The recent XMM-Newton observations of nearby cooling flow clusters revealed that the temperature gradient is not very large and is approximately $r^{-0.2}$ (Böhringer et al. (2001); Tamura et al. (2001)). These indicate that cooling is not as efficient as the standard cooling flow predictions. However a small temperature gradient of the gas could cause differences in the gas density distribution and the underlying potential distribution. We need further investigation to clarify through which physical processes such discrete cluster structures are formed.

We are grateful to M. Hattori and S. Sasaki for useful comments. We thank Philip Edwards for his careful review of the manuscript. N.O. is supported by a Research Fellowship for Young Scientists from the JSPS.

REFERENCES

- Allen, S.W., 1998, MNRAS, 296, 392.
- Böhringer, H., Belsole, E., Kennea, J., Matsushita, K., Molendi, S., Worrall, D.M., Mushotzky, R.F., Ehle, M., Guainazzi, M., Sakelliou, I., Stewart, G., Vestrand, W.T., Dos Santos, S., 2001, A&A, 365, L181.
- Buote, D.A., & Tsai, J.C., 1996, ApJ, 458, 27.
- Cavaliere, A., & Fusco-Femiano, R., 1976, A&A, 49, 137.
- Edge, A.C, Stewart, G.C., Fabian, A.C., & Arnaud, K. A., 1990, MNRAS, 245, 559.
- Ettori, S., & Fabian, A.C., 1999, MNRAS, 305, 834.
- Ezawa, H., Fukazawa, Y., Makishima, K., Ohashi, T., Takahara, F., Hu, X., & Yamasaki, N.Y., 1997, ApJ, 490, L33.
- Fabian, A.C., 1994, ARA&A, 32, 277.
- Fabian, A.C., Crawford, C.S., Edge, A.C., Mushotzky, R.F., 1994, MNRAS, 267, 779.
- Fujita, Y., & Takahara, F., 1999a, ApJ, 519, L51.
- Fujita, Y., & Takahara, F., 1999b, ApJ, 519, L55.
- Fukazawa, Y., Ishida, M., & Ebisawa, K., 1997, ASCANews Letter No.5.
- Hashimoto-dani, K., 1999, Ph.D. Dissertation, Osaka University.
- Mitsuda, K., & Ota, N., 2002, in preparation.
- Mohr, J.J., Evrard, A.E., Fabricant, D.G., & Geller, M.J., 1995, ApJ, 447, 8.
- Mohr, J.J., Mathiesen, B., & Evrard, A.E., 1999, ApJ, 517, 627.
- Ota, N., 2001, Ph.D. thesis, University of Tokyo (ISAS Research Note No.727).
- Prestwitch, A.H., Silverman, J., McDowell, J., Callanan, P., Snowden, S., 1998, Spectral Calibration of the ROSAT HRI (http://www.harvard.edu/rosat/rsdc_www/HRISPEC/spec_calib.html).
- Raymond, J.C., & Smith, B.W., 1977, ApJS, 35, 419.
- Snowden, S.L., 1998, ApJS, 117, 233.

Tamura, T., Kaastra, J.S., Peterson, J.R., Paerels, F.B.S., Mittaz, J.P.D., Trudolyubov, S.P., Stewart, G., Fabian, A.C., Mushotzky, R.F., Lumb, D.H., & Ikebe, Y, 2001, *A&A*, 365, 87.

Yaqoob, T., 1999, *ApJ*, 511, L75.

Zimmermann, H.-U., Belloni, T., Boese, G., Izzo, C., Kahabka, P., & Schwentkey, O., 1992, in V. Di. Gesu, L. Scarsi, R. Buccheri, P. Crane, M. Maccarone, and H.-U. Zimmermann (eds.), *Data Analysis in Astronomy IV*, pp 141-144, Plenum Press, New York and London.

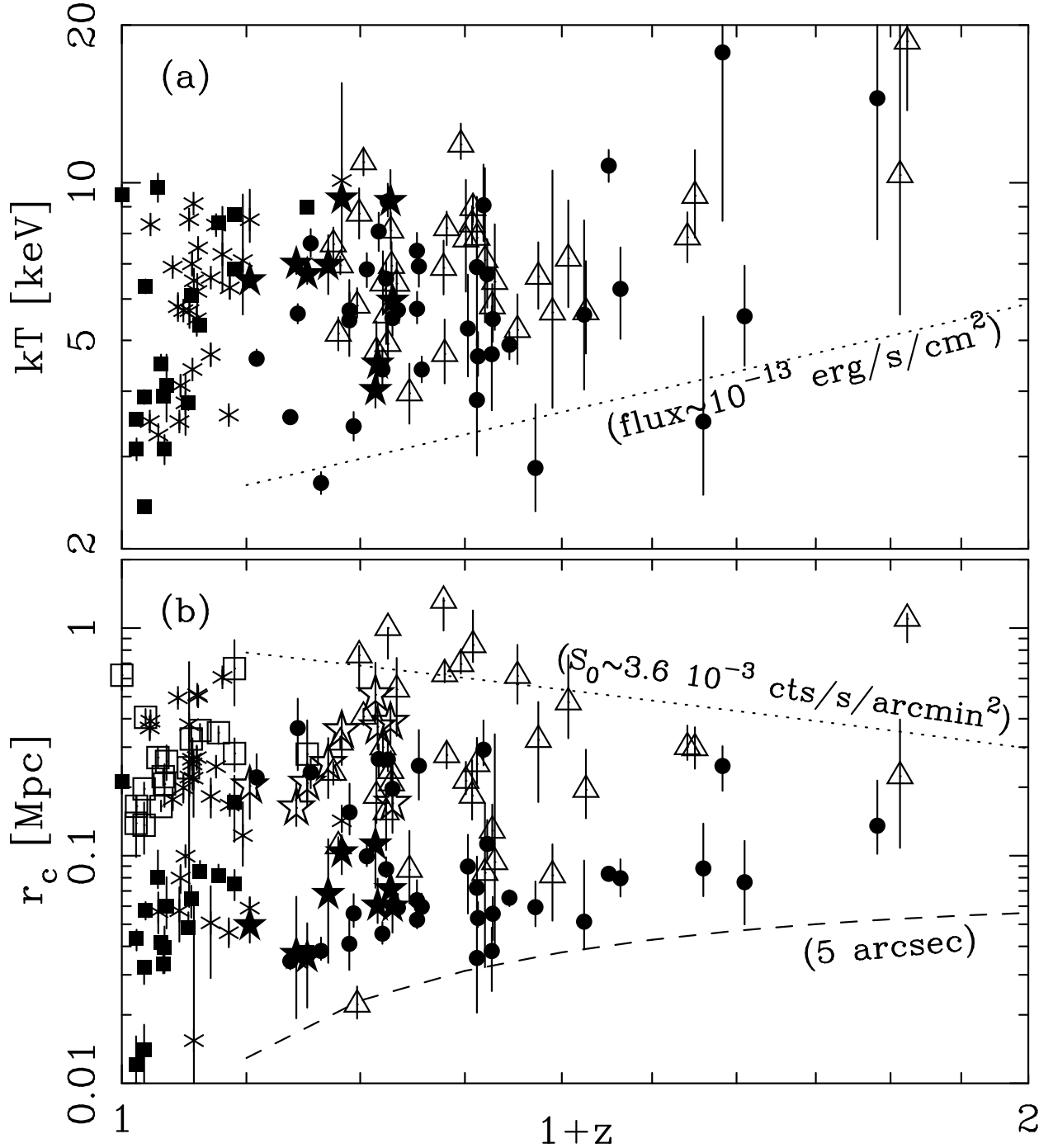


Fig. 1.— Redshift dependence of the average temperature (a) and the core radius (b). Subgroups of clusters are denoted with different symbols, the single β regular and irregular clusters (circles and triangles), the double β clusters (stars) where the core radii of two components are plotted with open and filled stars in panel (b), the single and double β clusters of nearby samples by Mohr, Mathiesen, & Evrard (1999) (asterisks and open/filled squares). The errors are at 90% confidence. The upper curve in panel (b) corresponds to a constant central surface brightness of $S_0 = 3.6 \times 10^{-3}$ counts/s/arcmin², which is the typical sensitivity of the present observations. In order to draw the curve, we assumed $\beta = 0.7$ and $kT = 5$ keV.

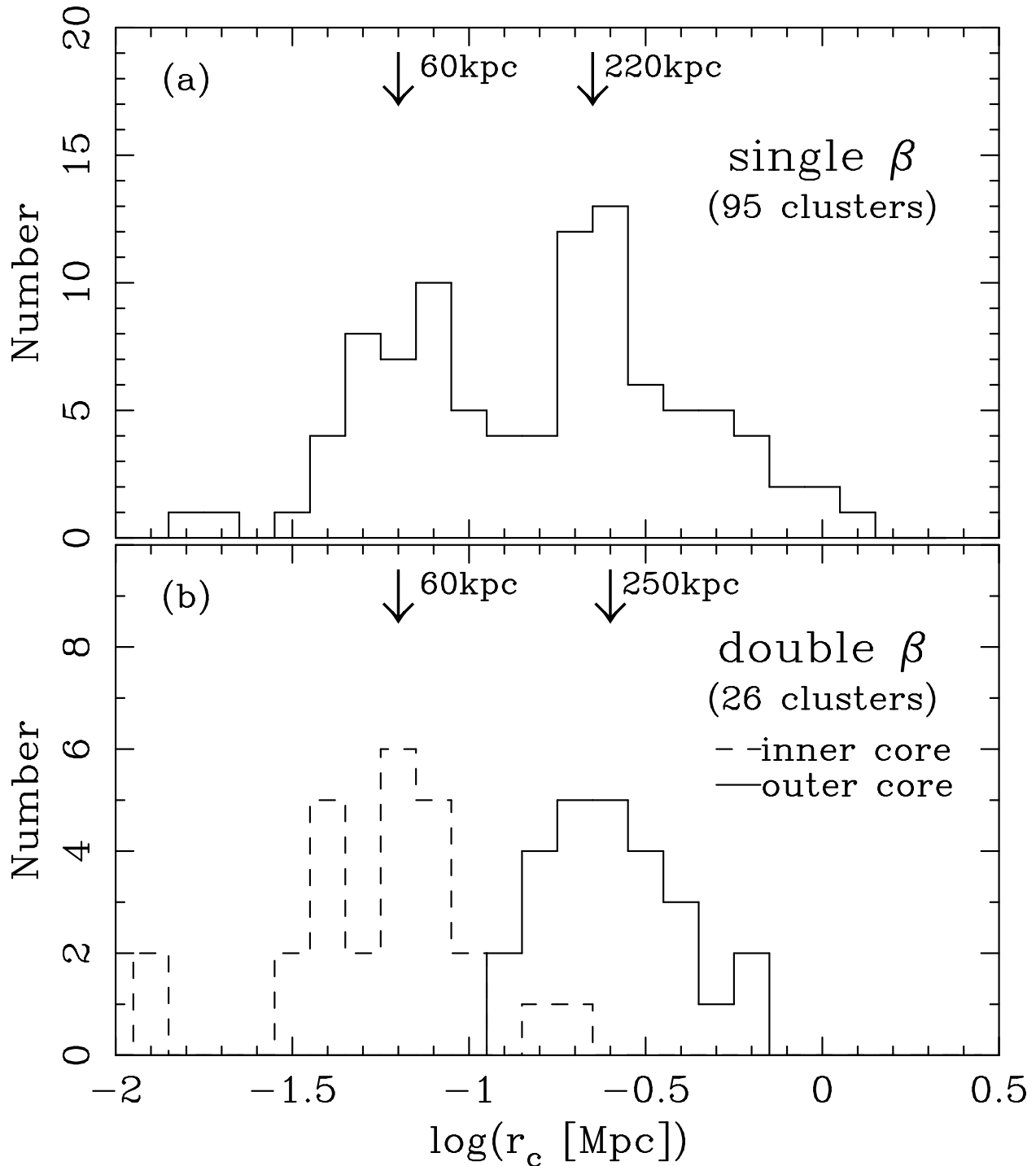


Fig. 2.— Histograms of the core radius for the single- β clusters (a) and the double- β clusters (b). Our distant ($z > 0.1$) sample and the nearby sample of Mohr, Mathiesen, & Evrard (1999) are added together. For the double- β clusters, the inner and the outer components are plotted separately with the solid and dashed lines.

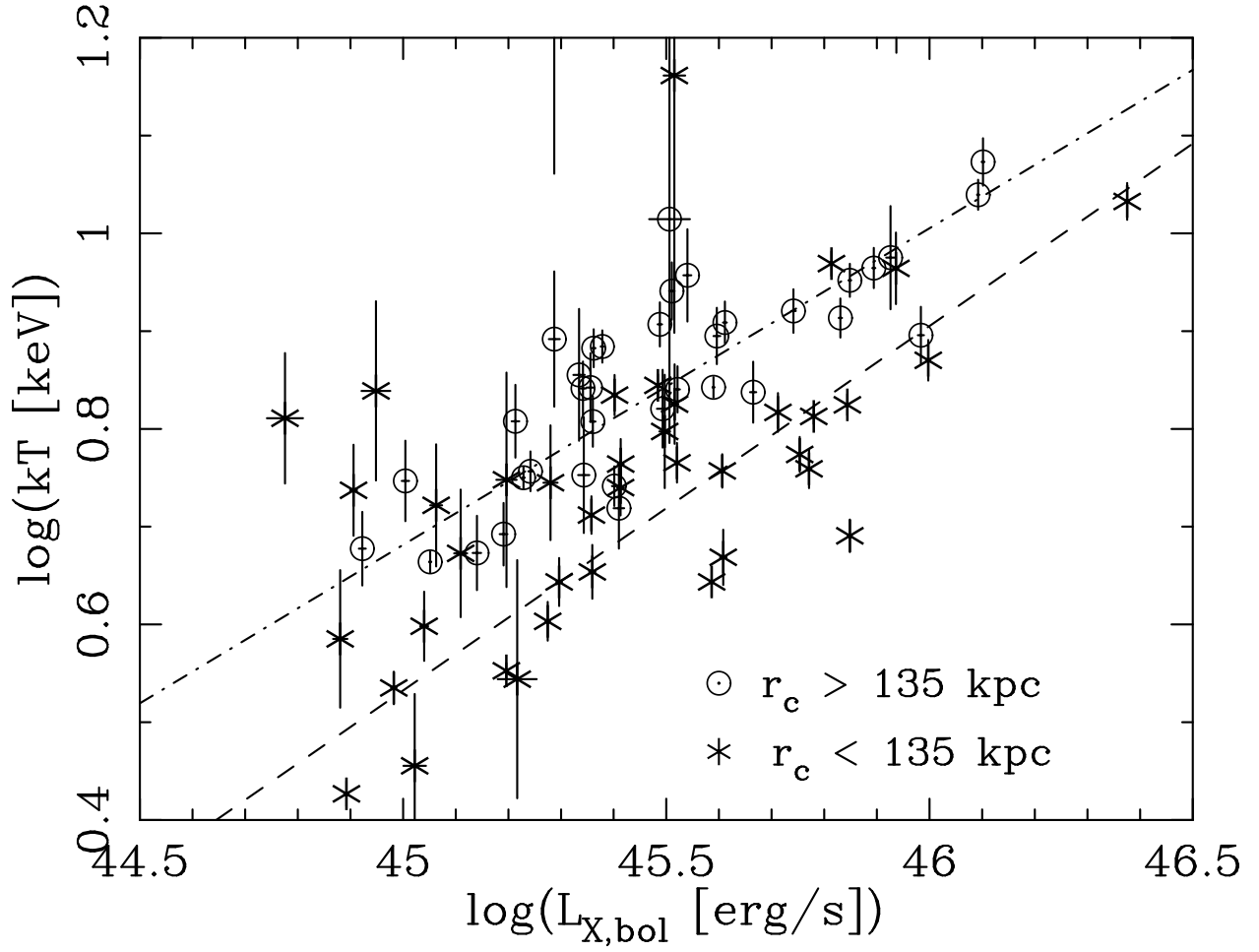


Fig. 3.— Luminosity-temperature relations derived from the ASCA observations of the distant clusters. The asterisks and the circles denote the clusters with $r_c < 135$ and $r_c > 135$ kpc, respectively. The vertical and horizontal error bars are the 1σ errors. The best-fit power-law functions are shown with the dashed and dot-dashed lines for the two subgroups.